Cytotoxicities and Quantitative Structure Activity Relationships of B13 Sulfonamides in HT-29 and A549 Cells

Seul Ki Chan Lee, Sang Min Park, and Chaeuk Im

College of Pharmacy, Chung-Ang University, Seoul 156-756, Korea

B13 analogues are being considered as therapeutic agents for cancer cells, since B13 is a ceramide analogue and inhibits ceramidase to promote apoptosis in cancer cells. B13 sulfonamides are assumed to have biological activity similar to B13, since they are made by bioisosterically substituting the carboxyl moiety of B13 with sulfone group. Twenty B13 sulfonamides were evaluated for their *in vitro* cytotoxicities against human colon cancer HT-29 and lung cancer A549 cell lines using MTT assays. Replacement of the amide group with a sulfonamide group increased cytotoxicity in both cancer cell lines. The sulfonamides with long alkyl chains exhibited activities two to three times more potent than that of B13 and compound (15) had the most potent activity with IC_{50} values of 27 and 28.7 μM for HT-29 and A549, respectively. The comparative molecular field analysis (CoMFA) and comparative molecular similarity indices analysis (CoMSIA) were used to carry out QSAR molecular modeling of these compounds. The predictive CoMSIA models for HT-29 and A549 gave cross-validated q2 values of 0.703 and 0.830, respectively. From graphical analysis of these models, we suppose that the stereochemistry of 1,3-propandiol is not important for activity and that introduction of a sulfonamide group and long alkyl chains into B13 can increase cytotoxicity.

Key Words: B13, Ceramide, Cytotoxicity, QSAR, Sulfonamides

INTRODUCTION

Sphingolipids, such as ceramide and its metabolites, have recently been recognized as important compounds as secondary messengers involved in signal transduction. They activate ceramide-mediated phosphatases and kinases to stimulate the apoptotic pathways and inhibit cancer cell growth [1-3]. They are also involved in cell division, differentiation, inflammation, and smooth muscle cell relaxation [4-7]. Some anticancer agents were reported to induce intracellular ceramide accumulation [8], which led to cell cycle arrest and apoptosis in tumor cells [9-11]. However, cellular ceramide is rapidly removed by ceramide metabolizing enzymes like ceramidase.

Because ceramide induces apoptosis in cancer cells, ceramide analogues are being considered as therapeutic agents for cancer cells [12-17]. The introduction of a phenyl ring into the long alkyl chain moiety of ceramide as in D-e-MAPP was shown to enhance ceramidase inhibition and increase intracellular ceramide concentration [18,19]. The aromatic analogues of ceramide, such as D-e-MAPP

with 1S, 2R configuration and B13 with 1R, 2R configuration rather than 2S, 3R configuration of natural ceramide, inhibit ceramidase to induce apoptosis (Fig. 1). In this way, they exhibit potent cytotoxicity against various cancer cells including leukemia, colon, and prostate cancer cells [20-25]. Furthermore, B13 showed selective cytotoxicity toward malignant cells but not normal cells and prevented colon cancer cells from the transition to metastasis in a nude mouse model [9].

The amide group of ceramide can be isosterically replaced by urea or an amine group to increase inhibitory activity against ceramidase and to promote cytotoxicity [25]. The B13 sulfonamides are assumed to exhibit biological activities similar to that of B13, since they were made by bioisosterically substituting the carboxyl moiety in B13 with a sulfone group. Sulfonamides are also known to have various biological activities acting as hypoglycemic, diuretic, and antibacterial agents [26-28]. Recently, some sulfonamides have been reported to demonstrate anticancer activity [29-32].

As a continuation of our previous reported work [33] and as an extension of those findings, we report here on the cytotoxicities of twenty B13 sulfonamide analogues against human colon and lung cancer cell lines and evaluate the influence of the stereochemistry of 1,3-propandiol, the p-ni-

**ABBREVIATIONS:** MTT, 3-[4,5-dimethylthiazol-2-yl]-2,5-diphenyl-tetrazolium bromide; B13, (1R,2R)-D-*threo*-2-(N-Myristoylamino)-1-(4'-nitrophenyl)-1,3-propanediol; PBS, phosphate-buffered saline; pIC_{50}, −log IC_{50}; QSAR, quantitative structure activity relationship; CoMFA, comparative molecular field analysis; CoMSIA, comparative molecular similarity indices analysis.
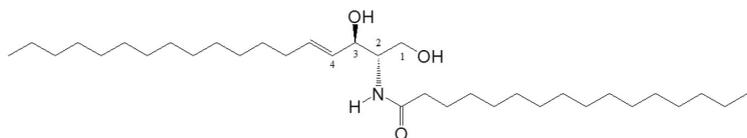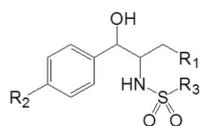
(2S,3R,4E)-D-e-Ceramide
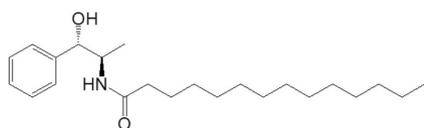
(1S,2R)-D-Mapp
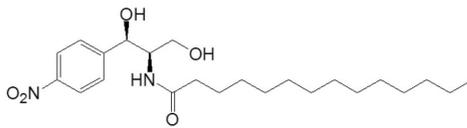
(1R,2R)-B13

Sulfonamide analogue of B13

Fig. 1. Structure of ceramide and B13 analogues.

tro group in the phenyl ring, and alkyl chain length in the sulfonamide moiety. We also carry out QSAR analysis to investigate the relationship between the structural features and cytotoxicity of B13 sulfonamide analogues.

METHODS

Chemicals

Phosphate-buffered saline (PBS) was bought from Boehringer Mannheim. Dimethyl sulfoxide (DMSO), 3-[4,5-dimethylthiazol-2-yl]-2,5-diphenyltetrazolium bromide (MTT), and other reagents were obtained from Sigma.

In vitro cytotoxic assay

The cytotoxic activities of B13 sulfonamides which were synthesized in our lab were estimated in two human tumor cell lines: colon cancer HT-29 and lung cancer A549. The results from the cytotoxic assays are illustrated in Table 1 and a description of the MTT-based colorimetric assay used is included in the legend for that Table [34].

Data sets and values

Twenty-one compounds were used to perform QSAR analysis. The molecular structures of the training and test sets are shown in Table 1. The data set was divided into two groups. Based on their different alkyl chain lengths and R, S configurations at C_1 and C_2, four compounds (1, 10, 12, 18) were selected for the test set, which was used for external validation of the QSAR models. The rest of the 17 compounds including B13 were used for the training set. All IC_{50} values were converted into pIC_{50} ($-\log IC_{50}$) values which were then used as the dependent values to derive

CoMFA and CoMSIA.

Molecular modeling

We used Sybyl-X 1.2 program for modeling molecules, performing partial least squares (PLS), and conducting CoMFA and CoMSIA [35]. Molecular structures were designed with a sketch tool and optimized using a TRIPOS force field with the Gasteiger Huckel charges and conjugated gradient method. The conformations with low energy were analyzed by simulated annealing and were aligned using the fitting atoms method. The propyl moiety (C_1-C_2-C_3) marked as a bold line in Table 1 was used as a common substructure and the most active compound (15) was used as a template molecule in alignment.

CoMFA and CoMSIA

CoMFA was executed in the steric and electrostatic fields with the default values. Aligned molecules were put into the three dimensional cubic lattice with a grid spacing of 2.0 Å. The energy cutoff was the default value of 30 kcal/mol. The Lennard-Jones potential and Coulombic potential were applied to calculate the steric and electrostatic field energies of CoMFA, respectively. The sp³ probe carbon atom with a charge of +1 and a Van der Waals radius of 1.52 Å was used to create the CoMFA steric and electrostatic fields. The CoMSIA concerns five properties (steric, electrostatic, hydrophobic, hydrogen bond acceptor, and hydrogen bond donor fields) using a common probe atom with radius 1.0 Å, charge +1, hydrophobicity +1, hydrogen bond donating +1, and hydrogen bond accepting +1.

Partial least square (PLS) analysis

In the PLS analysis, the leave-one-out method of cross-

Table 1. Structures and in vitro cytotoxicities of B13 sulfonamide analogues
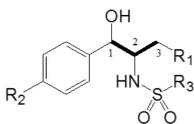
Compounds	R$_1$	R$_2$	R$_3$	Configuration	Cytotoxicity IC$_{50}$ (μM)	
					Colon cancer (HT-29)	Lung cancer (A549)
1	H	H	C$_7$H$_{15}$	1R, 2S	191.5	207.3
2	H	H	C$_8$H$_{17}$	1R, 2S	93.8	148.7
3	H	H	C$_9$H$_{19}$	1R, 2S	83.2	90.5
4	H	H	C$_{11}$H$_{23}$	1R, 2S	44.2	46.0
5	H	H	C$_{13}$H$_{27}$	1R, 2S	35.9	49.3
6	H	H	C$_7$H$_{15}$	1S, 2R	183.0	205.7
7	H	H	C$_8$H$_{17}$	1S, 2R	96.6	96.6
8	H	H	C$_9$H$_{19}$	1S, 2R	60.0	73.0
9	H	H	C$_{11}$H$_{23}$	1S, 2R	37.8	74.2
10	H	H	C$_{13}$H$_{27}$	1S, 2R	39.2	80.7
11	OH	NO$_2$	C$_7$H$_{15}$	1R, 2R	101.0	>267.3
12	OH	NO$_2$	C$_8$H$_{17}$	1R, 2R	53.3	84.6
13	OH	NO$_2$	C$_9$H$_{19}$	1R, 2R	27.9	42.7
14	OH	NO$_2$	C$_{11}$H$_{23}$	1R, 2R	25.7	41.1
15	OH	NO$_2$	C$_{13}$H$_{27}$	1R, 2R	27.0	28.7
16	OH	NO$_2$	C$_7$H$_{15}$	1S, 2S	161.6	267.3
17	OH	NO$_2$	C$_8$H$_{17}$	1S, 2S	100.3	89.0
18	OH	NO$_2$	C$_9$H$_{19}$	1S, 2S	52.2	69.1
19	OH	NO$_2$	C$_{11}$H$_{23}$	1S, 2S	61.3	40.9
20	OH	NO$_2$	C$_{13}$H$_{27}$	1S, 2S	30.8	30.8
B13				1R, 2R	68.4	94.2

The cells were plated at a density of approximately 1×10^4 cells/well in 96-well plates. Each well contained 180 μl of medium into which 20 μl of 10×concentration of prepared compounds or PBS were added. After 96h of culture, 0.1mg of MTT was added to each well and incubated at 37°C for 4 h. The plates were centrifuged at 450×g to precipitate the formazan crystals. The medium was removed and 150 μl of DMSO was added to each well to dissolve the formazan. In this assay, MTT was converted to blue formazan by mitochondrial dehydrogenase. The intensity of the blue color was measured with a microplate reader at a wavelength of 540 nm. The mean measured values are expressed as the IC$_{50}$, the concentration that reduced the optical density of the treated cells by 50% with respect to the untreated controls.

validation was carried out to determine the optimum number of components, which were then used for the non-cross-validated analysis. In the leave-one-out method, one compound was removed from the data set and its biological activity was predicted with the model derived from the rest of the data set.

RESULTS

In vitro cytotoxic activity

The cytotoxicities of twenty-one B13 sulfonamides against human colon cancer HT-29 and lung cancer A549 cell lines were estimated in vitro. Their biological activities are summarized in Table 1 and B13 itself showed moderate cytotoxicity with IC$_{50}$ values of 68.4 and 94.2 μM for HT-29 and A549 cells, respectively. In colon cancer HT-29 cells, most of the sulfonamides except for the short alkyl chain (C$_7$H$_{15}$ and C$_8$H$_{17}$) compounds (1, 2, 6, 7, 11, 16, 17) showed more potent activities than B13. The cytotoxicities of the long alkyl chain (C$_{13}$H$_{27}$) analogues (5, 10, 15, 20) were increased two times that of B13 to give IC$_{50}$ values of 35.9, 39.2, 27, and 30.8 μM, respectively, in HT-29 cells. Compounds (11~20) with a C$_3$-OH and para nitro group in the phenyl ring

had stronger activities than compounds (1~10) which did not have these groups. For lung cancer A549 cells, the long alkyl chain compounds exhibited more potent cytotoxicities than the short alkyl chain compounds. Some of the long alkyl chains (C$_{11}$H$_{23}$ and C$_{13}$H$_{27}$) analogues (4, 5, 14, 15, 19, 20) showed almost two-fold increases in activity with IC$_{50}$ values of 46, 49.3, 41.1, 28.7, 40.9, and 30.8 μM, respectively. Compounds (5, 10, 15, 20) with long alkyl chain (C$_{13}$H$_{27}$) were much more active than B13 against both tumor cell lines and exhibited IC$_{50}$ values of 35.9, 39.2, 27, and 30.8 μM, respectively, against colon cancer HT-29 cell lines and 49.3, 80.7, 28.7, and 30.8 μM, respectively, against lung cancer A549 cell lines. The IC$_{50}$ values of the other compounds ranged from 25.7 to 191.5 μM for HT-29 cells and 40.9 to 267.3 μM for A549 cells.

3D-QSAR analysis

The statistical data from CoMFA and CoMSIA models are illustrated in Table 2. All CoMFA and CoMSIA models were based on the training set of 17 compounds and the test set of 4 compounds.

Table 2. Statistical data of CoMFA and CoMSIA models

Field[a]	q^{2b}	N[c]	SEP[d]	r^2_{ncv}[e]	SEE[f]	F[g]	r^2_{pred}[h]	Contributions[a]				
								S	E	H	D	A
Colon cancer (HT-29 cells)												
CoMFA												
SE	0.198	3	0.273	0.987	0.035	329.619		0.446	0.554			
CoMSIA												
HD	0.701	4	0.173	0.985	0.039		198.589				0.605	0.395
HA	0.678	4	0.180	0.984	0.040	187.848				0.587		0.413
DA	0.444	3	0.227	0.935	0.078	62.026					0.400	0.600
SHA	0.556	4	0.211	0.991	0.030	327.721		0.249		0.444		0.307
EHA	0.495	4	0.225	0.988	0.035	247.728			0.365	0.398		0.237
HDA	**0.703**	**4**	**0.173**	**0.992**	**0.027**	**396.375**	**0.929**			**0.442**	**0.269**	**0.290**
Lung cancer (A549 cells)												
CoMFA												
SE	0.442	3	0.255	0.990	0.034	426.595		0.420	0.580			
CoMSIA												
EH	0.735	4	0.183	0.998	0.017	1,364.022			0.480	0.520		
EA	0.509	3	0.222	0.988	0.035	341.530			0.560			0.440
HA	**0.830**	**4**	**0.147**	**0.990**	**0.036**	**290.264**	**0.832**			**0.587**		**0.413**
SHA	0.705	4	0.193	0.992	0.032	373.955		0.223		0.456		0.321
EHA	0.772	4	0.170	0.997	0.019	1,033.608					0.319	0.681
HDA	0.777	4	0.168	0.992	0.031	382.732				0.496	0.190	0.314

[a]Fields used (S, steric; E, electrostatic; H, hydrophobic; D, H-bond donor; A, H-bond acceptor); [b]q^2, cross-validated correlation coefficient from leave-one-out (LOO); [c]N, optimum number of components; [d]SEP, standard error of prediction; [e]r^2_{ncv}, non-cross-validated correlation coefficient; [f]SEE, standard error of estimate; [g]F, F-test value; [h]r^2_{pred}, predicted correlation coefficient.

Table 3. Actual *versus* predicted cytotoxicities (pIC_{50}) of the training set

Compounds	Colon cancer cells (HT-29 cells)			Lung cancer cells (A549 cells)		
	Actual[a]	Predicted[b]	Residual[c]	Actual[a]	Predicted[b]	Residual[c]
2	4.03	4.03	0.00	3.83	3.83	0.00
3	4.08	4.10	−0.02	4.04	4.09	−0.05
4	4.36	4.38	−0.02	4.34	4.30	0.04
5	4.44	4.40	0.04	4.31	4.26	0.05
6	3.74	3.74	0.00	3.69	3.70	−0.01
7	4.01	4.03	−0.02	4.02	3.96	0.06
8	4.22	4.24	−0.02	4.14	4.14	−0.01
9	4.42	4.39	0.03	4.13	4.14	−0.01
11	4.00	4.02	−0.03	3.57	3.62	−0.04
13	4.55	4.53	0.03	4.37	4.37	0.00
14	4.59	4.59	0.00	4.39	4.42	−0.03
15	4.57	4.59	−0.02	4.54	4.55	0.00
16	3.79	3.75	0.04	3.57	3.55	0.02
17	4.00	4.02	−0.02	4.05	4.06	−0.01
19	4.21	4.19	0.02	4.39	4.42	−0.03
20	4.55	4.57	−0.02	4.51	4.51	0.00
B13	4.17	4.16	0.01	4.03	4.00	0.02
	Average		0.02			0.02

[a]Actual cytotoxic activity; [b]predicted activity by the CoMSIA model with hydrophobic, hydrogen bond donor, and hydrogen bond acceptor fields; [c]difference between the actual and predicted activities; The pIC_{50} ($-\log IC_{50}$) values were converted from IC_{50} values.

Colon cancer HT-29 cells

The CoMSIA model with hydrophobic, hydrogen bond donor, and hydrogen bond acceptor fields gave a cross-validated coefficient (q^2) value of 0.703 and non-cross-validated coefficient (r^2_{ncv}) value of 0.992 with the optimum number of components of 4; SEE, 0.027; and F value, 396.375. The q^2 value obtained from this model was higher than those from any other CoMFA and CoMSIA models. The predictive ability of the model was expressed as r^2_{pred} with a value of 0.929. The predicted pIC_{50} values and residuals for training and test sets are shown in Tables 3 and 4, respectively. A graph of actual *versus* predicted pIC_{50} values for the training and test sets is illustrated in Fig. 2.

Table 4. Actual versus predicted cytotoxicities (pIC$_{50}$) of the test set

Compounds	Colon cancer cells (HT-29 cells)			Lung cancer cells (A549 cells)		
	Actual[a]	Predicted[b]	Residual[c]	Actual[a]	Predicted[b]	Residual[c]
1	3.72	3.79	−0.07	3.68	3.72	−0.03
10	4.41	4.42	−0.01	4.09	4.23	−0.14
12	4.27	4.24	0.03	4.07	4.00	0.07
18	4.27	4.16	0.12	4.16	4.23	−0.07
	Average		0.06			0.08

[a]Actual cytotoxic activity; [b]predicted activity by the CoMSIA model with hydrophobic and hydrogen bond acceptor fields; [c]difference between the actual and predicted activities; The pIC$_{50}$ (−log IC$_{50}$) values were converted from IC$_{50}$ values.
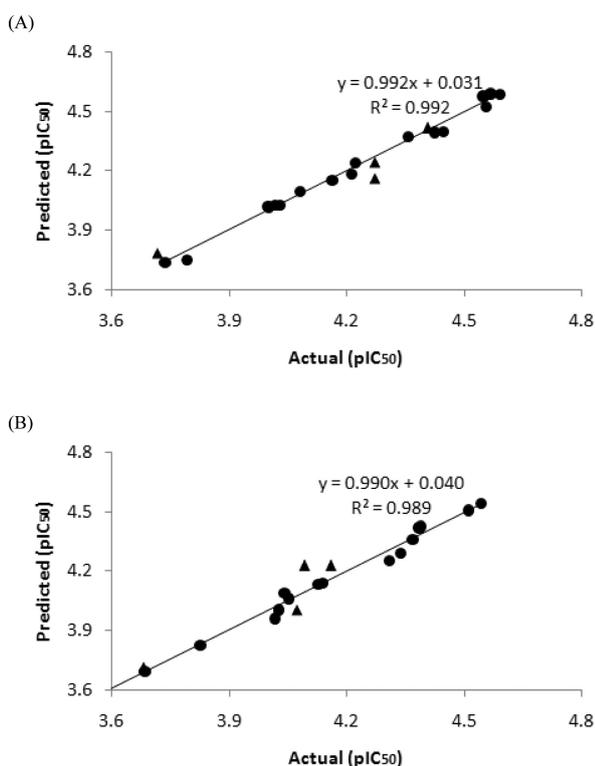
(A)

(B)

Fig. 2. Graph of the actual *versus* predicted activities for training and test set compounds. (A) Colon cancer HT-29 cells. (B) Lung cancer A549 cells. The IC$_{50}$ values were transformed into pIC$_{50}$ (−log IC$_{50}$) values (●: training set molecules, ▲: test set molecules).

Lung cancer A549 cells

The CoMSIA model with hydrophobic and hydrogen bond acceptor fields was used to calculate the cross-validated coefficient (q^2), non-cross-validated coefficient (r$^2_{ncv}$), and optimum number component (N) to give values of 0.830, 0.990, and 4, respectively. With this model, the predicted r^2 value (r$^2_{pred}$) was 0.832 and the predicted pIC$_{50}$ values and residuals of the training set and test set are summarized in Tables 3 and 4, respectively. Fig. 2B describes the correlation between the actual *versus* predicted pIC$_{50}$ values of the compounds in the training and test sets.

DISCUSSION

As described in the *in vitro* bioassay, compound (15) showed the most potent activity against both colon cancer HT-29 and lung cancer A549 cell lines with IC$_{50}$ values of 27.0 and 28.7 μM, respectively. B13 sulfonamides with a C$_{13}$H$_{27}$ alkyl chain (5, 15, 10, 20) showed two or three times more potent cytotoxicities than B13 which also had a C$_{13}$H$_{27}$ alkyl chain, suggesting that introduction of a sulfonamide group into B13 increased its cytotoxicity. The stereochemistry of 1,3-propandiol was not important for cytotoxicity in compounds with alkyl chains of the same length, although some (1R, 2R)-compounds (12, 13, 15) manifested stronger cytotoxicities than the (1S, 2S)-compounds (16, 18, 20), which had slightly more potent activities than the (1R, 2S)-compounds (2, 4, 5) and (1S, 2R)-compounds (7, 8, 9). The compounds with a *para* nitro group at the phenyl ring and a C$_3$-OH group (13, 15, 18, 20) demonstrated higher activities than the compounds without them (3, 5, 8, 10). In general, compounds with long alkyl chains (5, 10, 15, 20) exhibited enhanced activity compared to those with short alkyl chains (1, 6, 11, 16). This finding was consistent with the reported trend that cytotoxicity increased with an increase in the acyl chain length of ceramide [36].

In the CoMSIA model of colon cancer HT-29 cells, the cross-validated coefficient (q^2) value was 0.703 and was considered sufficiently predictive for validation because it was greater than 0.6. The relative contributions of the hydrophobic field (44.2%), hydrogen bond donor field (26.9%), and hydrogen bond acceptor field (29%) indicated that the phenyl ring and long alkyl chain for hydrophobicity, the hydrogen atom of sulfonamide as a hydrogen bond donor, oxygen atoms of the C$_1$-OH and sulfone group as hydrogen bond acceptors contributed to cytotoxicity. For lung cancer A549, the CoMSIA model with hydrophobic and hydrogen bond acceptor fields yielded high q^2 (0.830) and r$^2_{ncv}$ (0.990) values which represented a precise predictivity for this model. The contributions of the hydrophobic field (58.7%) and hydrogen bond acceptor field (41.3%) indicated that strong hydrophobic ligand-receptor interactions were involved in the cytotoxicities of the compounds. The small average residual values (0.02) between actual and predicted activities in Table 3 demonstrated that the predicted activity from the CoMSIA models correlated well with actual activity. The test set was used to validate the predictive ability of these CoMSIA models and their small average residual values (0.06 and 0.08) showed that both models accurately predicted the cytotoxicities of test set molecules.

The CoMSIA contour maps illustrate the structural features important for potent activity to show regions around
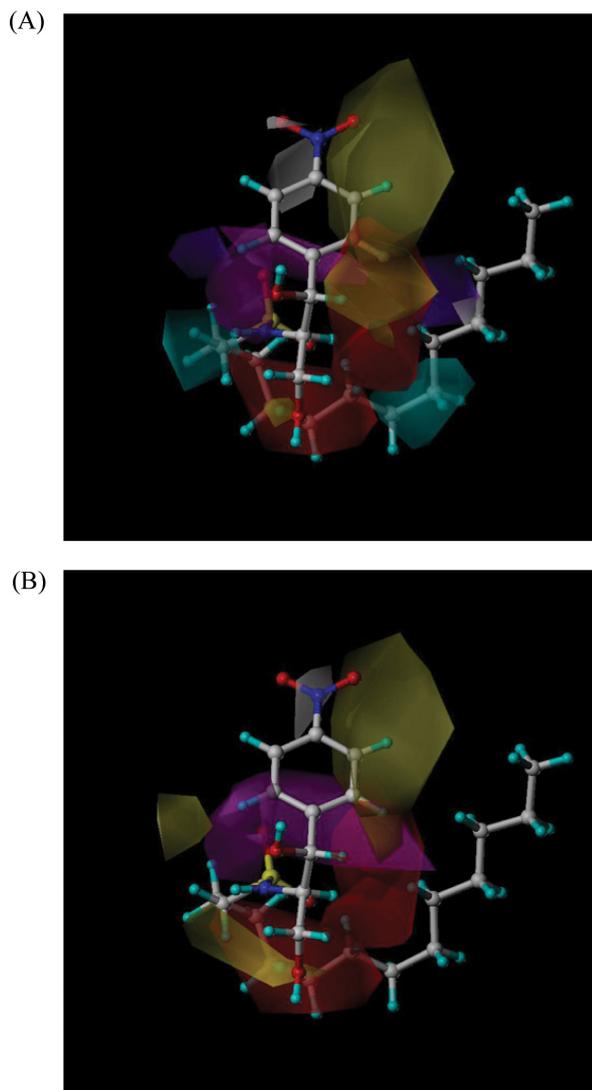
(A)

(B)

Fig. 3. 3D-contour maps of CoMSIA models. (A) CoMSIA model with hydrophobic, hydrogen bond donor, and hydrogen bond acceptor fields for colon cancer HT-29 cells. (B) CoMSIA model with hydrophobic and hydrogen bond acceptor fields for lung cancer A549 cells. Compound (15) is shown within the fields (yellow, favorable hydrophobicity; white, unfavorable hydrophobicity; cyan, favorable hydrogen bond donor; purple, unfavorable hydrogen bond donor; magenta, favorable hydrogen bond acceptor; red, unfavorable hydrogen bond acceptor).

molecules, in which increased or decreased activity was expected by physicochemical property changes. In Fig. 3, the yellow contours indicate regions where a hydrophobic group would increase the biological activity, whereas the white ones would decrease the activity.

The cyan and purple contours denote the places where a hydrogen bond donor would be favorable and unfavorable, respectively. The magenta regions represent areas that are favorable for a hydrogen bond acceptor, while red regions indicate areas unfavorable for such a group. The molecule used in the contour maps is compound (15), which showed the most potent cytotoxicity.

The CoMSIA contour map of colon cancer HT-29 cells (Fig. 3A) presents yellow contours at *ortho* and *meta* positions of the phenyl ring. These yellow contours suggest that hydrophobic groups at these regions would enhance cytotoxicity and that the introduction of a naphthyl ring instead of a phenyl ring would increase activity. This finding was supported by the compounds (1, 6, 11) in which yellow contours were superimposed with oxygen atoms of sulfonamide and C_1-OH groups to show much lower activities than other compounds with IC_{50} values of 191.5, 183, and 101 μM, respectively. The cyan contours near the hydrogen atoms of sulfonamide in compounds (5, 15) and the C_3-OH group in compound (20) coincided with regions favorable for a hydrogen bond donor and the magenta contours around the oxygen atoms of the C_1-OH and sulfonamide groups in compounds (5, 15, 20) corresponded to favorable hydrogen bond acceptor regions helping to account for their high potency. The CoMSIA contour map of lung cancer A549 cells (Fig. 3B) illustrated yellow contours at *ortho* and *meta* positions of the phenyl ring and the alkyl chain in compounds (5, 15, 20), where they were in accord with hydrophobically favorable regions to produce strong cytotoxic activities. It was also shown that the favorable hydrogen bond acceptor regions (magenta contour) were near the oxygen atoms of C_1-OH and sulfonamide groups, while unfavorable regions (red contour) were located around the alkyl side chain in compounds (5, 15, 20). These regions correlated well with the contour map to explain their potent cytotoxicity.

In conclusion, compounds (5, 15, 20) exhibited stronger cytotoxicities than B13 in both tumor cell lines. The good predictivity of the CoMSIA models was illustrated by high q^2 (0.703 and 0.830) and r^2_{ncv} (0.992 and 0.990) coefficient values. The small average residual values of the training (0.02) and test (0.06 and 0.08) sets indicated that the predicted activities from CoMSIA models correlated well with the actual activities. Cytotoxic assays demonstrated that the stereochemistry of 1,3-propanediol was not important for activity and that a sulfonamide group and long alkyl chain increased the cytotoxicity of the compounds. Furthermore, the introduction of a naphthyl ring in place of the phenyl ring was suggested to increase hydrophobicity and cytotoxicity.

ACKNOWLEDGMENTS

REFERENCES

1. **Hannun YA.** Functions of ceramide in coordinating cellular responses to stress. *Science.* 1996;274:1855-1859.
2. **Haimovitz-Friedman A, Kolesnick RN, Fuks Z.** Ceramide signaling in apoptosis. *Br Med Bull.* 1997;53:539-553.
3. **Fillet M, Bentires-Alj M, Deregowski V, Greimers R, Gielen J, Piette J, Bours V, Merville MP.** Mechanisms involved in exogenous C2- and C6-ceramide-induced cancer cell toxicity. *Biochem Pharmacol.* 2003;65:1633-1642.
4. **Kim HJ, Song JY, Park HJ, Park HK, Yun DH, Chung JH.** Naringin Protects against Rotenone-induced Apoptosis in Human Neuroblastoma SH-SY5Y Cells. *Korean J Physiol Pharmacol.* 2009;13:281-285.
5. **Hannun YA, Obeid LM.** The Ceramide-centric universe of lipid-mediated cell regulation: stress encounters of the lipid

kind. *J Biol Chem.* 2002;277:25847-25850.

6. **Hanada K, Kumagai K, Yasuda S, Miura Y, Kawano M, Fukasawa M, Nishijima M.** Molecular machinery for non-vesicular trafficking of ceramide. *Nature.* 2003;426:803-809.

7. **Lee DW, Park SY, Ryu JS, Kim SH, Im CU, Choi SH, Lee SE, Ko SK, Sohn UD.** Relaxation effect of synthetic ceramide analogues in cat esophageal smooth muscle cells. *Korean J Physiol Pharmacol.* 2008;12:137-142.

8. **Eto M, Bennouna J, Hunter OC, Hershberger PA, Kanto T, Johnson CS, Lotze MT, Amoscato AA.** C16 ceramide accumulates following androgen ablation in LNCaP prostate cancer cells. *Prostate.* 2003;57:66-79.

9. **Selzner M, Bielawska A, Morse MA, Rüdiger HA, Sindram D, Hannun YA, Clavien PA.** Induction of apoptotic cell death and prevention of tumor growth by ceramide analogues in metastatic human colon cancer. *Cancer Res.* 2001;61:1233-1240.

10. **Liu X, Elojeimy S, El-Zawahry AM, Holman DH, Bielawska A, Bielawski J, Rubinchik S, Guo GW, Dong JY, Keane T, Hannun YA, Tavassoli M, Norris JS.** Modulation of ceramide metabolism enhances viral protein apoptin's cytotoxicity in prostate cancer. *Mol Ther.* 2006;14:637-646.

11. **Senchenkov A, Litvak DA, Cabot MC.** Targeting ceramide metabolism--a strategy for overcoming drug resistance. *J Natl Cancer Inst.* 2001;93:347-357.

12. **Dindo D, Dahm F, Szulc Z, Bielawska A, Obeid LM, Hannun YA, Graf R, Clavien PA.** Cationic long-chain ceramide LCL-30 induces cell death by mitochondrial targeting in SW403 cells. *Mol Cancer Ther.* 2006;5:1520-1529.

13. **Senkal CE, Ponnusamy S, Rossi MJ, Sundararaj K, Szulc Z, Bielawski J, Bielawska A, Meyer M, Cobanoglu B, Koybasi S, Sinha D, Day TA, Obeid LM, Hannun YA, Ogretmen B.** Potent antitumor activity of a novel cationic pyridinium-ceramide alone or in combination with gemcitabine against human head and neck squamous cell carcinomas *in vitro* and *in vivo. J Pharmacol Exp Ther.* 2006;317:1188-1199.

14. **Bedia C, Triola G, Casas J, Llebaria A, Fabriàs G.** Analogs of the dihydroceramide desaturase inhibitor GT11 modified at the amide function: synthesis and biological activities. *Org Biomol Chem.* 2005;3:3707-3712.

15. **Granot T, Milhas D, Carpentier S, Dagan A, Ségui B, Gatt S, Levade T.** Caspase-dependent and -independent cell death of Jurkat human leukemia cells induced by novel synthetic ceramide analogs. *Leukemia.* 2006;20:392-399.

16. **Morales A, París R, Villanueva A, Llacuna L, García-Ruiz C, Fernández-Checa JC.** Pharmacological inhibition or small interfering RNA targeting acid ceramidase sensitizes hepatoma cells to chemotherapy and reduces tumor growth *in vivo. Oncogene.* 2007;26:905-916.

17. **Nam EJ, Lee HS, Lee YJ, Joo WS, Maeng SH, Im HI, Park CW, Kim YS.** Ceramide is involved in MPP+-induced cytotoxicity in human neuroblastoma cells. *Korean J Physiol Pharmacol.* 2002;6:281-286.

18. **Raisova M, Goltz G, Bektas M, Bielawska A, Riebeling C, Hossini AM, Eberle J, Hannun YA, Orfanos CE, Geilen CC.** Bcl-2 overexpression prevents apoptosis induced by ceramidase inhibitors in malignant melanoma and HaCaT keratinocytes. *FEBS Lett.* 2002;516:47-52.

19. **Selzner M, Bielawska A, Morse MA, Rüdiger HA, Sindram D, Hannun YA, Clavien PA.** Induction of apoptotic cell death and prevention of tumor growth by ceramide analogues in metastatic human colon cancer. *Cancer Res.* 2001;61:1233-1240.

20. **Alphonse G, Bionda C, Aloy MT, Ardail D, Rousson R, Rodriguez-Lafrasse C.** Overcoming resistance to gamma-rays

in squamous carcinoma cells by poly-drug elevation of ceramide levels. *Oncogene.* 2004;23:2703-2715.

21. **Lépine S, Lakatos B, Courageot MP, Le Stunff H, Sulpice JC, Giraud F.** Sphingosine contributes to glucocorticoid-induced apoptosis of thymocytes independently of the mitochondrial pathway. *J Immunol.* 2004;173:3783-3790.

22. **Bielawska A, Greenberg MS, Perry D, Jayadev S, Shayman JA, McKay C, Hannun YA.** (1S,2R)-D-erythro-2-(N-myristoylamino)-1-phenyl-1-propanol as an inhibitor of ceramidase. *J Biol Chem.* 1996;271:12646-12654.

23. **Samsel L, Zaidel G, Drumgoole HM, Jelovac D, Drachenberg C, Rhee JG, Brodie AM, Bielawska A, Smyth MJ.** The ceramide analog, B13, induces apoptosis in prostate cancer cell lines and inhibits tumor growth in prostate cancer xenografts. *Prostate.* 2004;58:382-393.

24. **Holman DH, Turner LS, El-Zawahry A, Elojeimy S, Liu X, Bielawski J, Szulc ZM, Norris K, Zeidan YH, Hannun YA, Bielawska A, Norris JS.** Lysosomotropic acid ceramidase inhibitor induces apoptosis in prostate cancer cells. *Cancer Chemother Pharmacol.* 2008;61:231-242.

25. **Usta J, El Bawab S, Roddy P, Szulc ZM, Yusuf, Hannun A, Bielawska A.** Structural requirements of ceramide and sphingosine based inhibitors of mitochondrial ceramidase. *Biochemistry.* 2001;40:9657-9668.

26. **Boyd AE 3rd.** Sulfonylurea receptors, ion channels, and fruit flies. *Diabetes.* 1988;37:847-850.

27. **Maren TH.** Relatons between structure and biological activity of sulfonamides. *Annu Rev Pharmacol Toxicol.* 1976;16:309-327.

28. **Drews J.** Drug discovery: a historical perspective. *Science.* 2000;287:1960-1964.

29. **Abbate F, Casini A, Owa T, Scozzafava A, Supuran CT.** Carbonic anhydrase inhibitors: E7070, a sulfonamide anticancer agent, potently inhibits cytosolic isozymes I and II, and transmembrane, tumor-associated isozyme IX. *Bioorg Med Chem Lett.* 2004;14:217-223.

30. **Ghorab MM, Noaman E, Ismail MM, Heiba HI, Ammar YA, Sayed MY.** Novel antitumor and radioprotective sulfonamides containing pyrrolo [2,3-d]pyrimidines. *Arzneimittelforschung.* 2006;56:405-413.

31. **Rostom SA.** Synthesis and in vitro antitumor evaluation of some indeno[1,2-c]pyrazol(in)es substituted with sulfonamide, sulfonylurea(-thiourea) pharmacophores, and some derived thiazole ring systems. *Bioorg Med Chem.* 2006;14:6475-6485.

32. **Supuran CT, Casini A, Mastrolorenzo A, Scozzafava A.** COX-2 selective inhibitors, carbonic anhydrase inhibition and anticancer properties of sulfonamides belonging to this class of pharmacological agents. *Mini Rev Med Chem.* 2004;4:625-632.

33. **Kim YJ, Kim EA, Sohn UD, Yim CB, Im C.** Cytotoxic activity and structure activity relationship of ceramide analogues in Caki-2 and HL-60 cells. *Korean J Physiol Pharmacol.* 2010;14:441-447.

34. **Park JG, Kramer BS, Steinberg SM, Carmichael J, Collins JM, Minna JD, Gazdar AF.** Chemosensitivity testing of human colorectal carcinoma cell lines using a tetrazolium-based colorimetric assay. *Cancer Res.* 1987;47:5875-5879.

35. **SYBYL Molecular Modeling Software.** USA: Tripos Inc., St. Louis; 2010.

36. **Chang YT, Choi J, Ding S, Prieschl EE, Baumruker T, Lee JM, Chung SK, Schultz PG.** The synthesis and biological characterization of a ceramide library. *J Am Chem Soc.* 2002;124:1856-1857.